

A single-molecule approach to DNA replication in *Escherichia coli* cells demonstrated that DNA polymerase III is a major determinant of fork speed

Tuan Minh Pham,¹ Kang Wei Tan,¹
Yuichi Sakumura,^{1,2} Katsuzumi Okumura,³
Hisaji Maki¹ and Masahiro Tatsumi Akiyama^{1*}

¹Division of Systems Biology, Graduate School of Biological Sciences, Nara Institute of Science and Technology, 8916-5 Takayama, Ikoma, Nara 630-0192, Japan.

²Department of Information Science and Technology, Aichi Prefectural University, Nagakute, Aichi 480-1198, Japan.

³Department of Life Science, Graduate School of Bioresources, Mie University, Tsu, Mie 514-8507, Japan.

Summary

The replisome catalyses DNA synthesis at a DNA replication fork. The molecular behaviour of the individual replisomes, and therefore the dynamics of replication fork movements, in growing *Escherichia coli* cells remains unknown. DNA combing enables a single-molecule approach to measuring the speed of replication fork progression in cells pulse-labelled with thymidine analogues. We constructed a new thymidine-requiring strain, eCOMB (*E. coli* for combing), that rapidly and sufficiently incorporates the analogues into newly synthesized DNA chains for the DNA-combing method. In combing experiments with eCOMB, we found the speed of most replication forks in the cells to be within the narrow range of 550–750 nt s⁻¹ and the average speed to be 653 ± 9 nt s⁻¹ (± SEM). We also found the average speed of the replication fork to be only 264 ± 9 nt s⁻¹ in a *dnaE173*-eCOMB strain producing a mutant-type of the replicative DNA polymerase III (Pol III) with a chain elongation rate (300 nt s⁻¹) much lower than that of the wild-type Pol III (900 nt s⁻¹). This indicates that the speed of chain elongation by Pol III is a

major determinant of replication fork speed in *E. coli* cells.

Introduction

Escherichia coli has served as the leading model system for clarifying the molecular mechanisms underlying DNA replication (Kornberg and Baker, 1992). Replication of double-stranded DNA (dsDNA) is carried out by the replisome, the multi-protein complex formed at a Y-shaped DNA replication fork. The key components of the *E. coli* replisome are DnaB helicase, DnaG primase, and the replicative DNA polymerase III (Pol III) holoenzyme (O'Donnell, 2006; McHenry, 2011). The co-ordinated functions of these components define the replisome action and, thereby, the replication fork movements on the *E. coli* chromosome.

The functional replisome that catalyses synthesis of the leading and lagging strands concurrently can be reconstituted from purified proteins including the three key components by using the *oriC* plasmid (Funnell *et al.*, 1986; Higuchi *et al.*, 2003) and the rolling-circle DNA replication systems (Wu *et al.*, 1992; McInerney and O'Donnell, 2004). Pol III and DnaB are progressive molecular motors that move on single-stranded DNA (ssDNA). Since the DNA unwinding rate of DnaB helicase (35 nt s⁻¹) is much slower than the DNA chain elongation rate of Pol III (900 nt s⁻¹) and the strand displacement by Pol III is weak (Kim *et al.*, 1996; Sugaya *et al.*, 2002), it has been postulated that elongation of the leading strand could act as the pacemaker of replication fork progression such that Pol III pushes DnaB in the replisome (Patel *et al.*, 2011). Recently, the real-time observation of a single molecule has been applied to study the dynamic behaviour of individual *E. coli* replisomes reconstituted in the rolling-circle DNA replication systems *in vitro* (van Oijen and Loparo, 2010). One experiment showed that at 37°C the fork speed ranged from 200 to 1000 nt s⁻¹ with a mean speed of 536 nt s⁻¹ (Tanner *et al.*, 2009). In experiments at 23°C, the varying speeds for 112 replisomes were fitted to a single Gaussian function with a mean rate of 246 nt s⁻¹ (Yao *et al.*, 2009).

Accepted 27 August, 2013. *For correspondence. E-mail akiyamam@bs.naist.jp; Tel. (+81) 743 72 5491; Fax (+81) 743 72 5499.

The fork speed in *E. coli* cells was estimated to be about 800 nt s⁻¹ when the estimate was based on the roughly 50 min duplication time (the C period) determined for a 4.6 Mb genome by flow cytometry (Atkinson *et al.*, 2011) and cell cycle parameter analysis (Odsbu *et al.*, 2009). Slightly lower speeds, 550–750 nt s⁻¹, were determined by gene dosage analysis with a genomic microarray (Khodursky *et al.*, 2000; Breier *et al.*, 2005; Tehranchi *et al.*, 2010). These values, however, are average fork speeds and thus obscure the variation of individual molecules. It is not easy to obtain an accurate value for fork speed and assess the fine dynamics of individual replisomes on the *E. coli* chromosome. In addition, the extent to which the fork speed varies during chromosomal DNA replication in the cell remains unknown. The fork speed may be reduced when the replisome encounters various natural obstacles on the chromosome (Mirkin and Mirkin, 2007). As in the case of *in vitro* reconstituted replisomes, the single-molecule approach would be a good way to investigate the replication-fork movement in living cells. It seems very difficult, however, to use a real-time measurement to investigate the behaviour of individual replication forks in *E. coli* cells because the chromosomal DNA in the small cell is extremely condensed. Instead, a direct measurement of the length of DNA newly synthesized in a given time may be applicable. From this reason, we developed a DNA-combing method for chromosomal DNA pulse-labelled in growing *E. coli* cells.

Molecular DNA combing is a single-molecule approach used to examine chromosomal DNA that has been pulse-labelled with halogenated analogues of thymidine such as 5-Bromo-2'-deoxyuridine (BrdU), 5-Chloro-2'-deoxyuridine (CldU) and 5-Iodo-2'-deoxyuridine (IdU) during DNA replication (Bensimon *et al.*, 1994; Bianco *et al.*, 2012). Replication dynamics in eukaryotic cells have been successfully investigated with DNA combing (Sugimura *et al.*, 2008). Since the labelled DNA is stretched on a glass surface and visualized under a microscope, the field of view restricts the measurable DNA length to below 300 kb. This limitation means that in *E. coli* cells the pulse-labelling with the analogues needs to be done in less than 6 min because the average rate of DNA synthesis in *E. coli* cells is 800 nt s⁻¹. In an earlier report, Breier *et al.* stated that thymidine-auxotroph derivatives of the wild-type K12 strains were not satisfactory for incorporation of BrdU into chromosomal DNA (Breier *et al.*, 2005). Even when Breier *et al.* used the non-K12 strain 15T⁻, which is known to incorporate extracellular thymidine efficiently (Roepke *et al.*, 1944), the technique allowed visualization of replicated DNA only after 10–15 min of labelling with BrdU (Breier *et al.*, 2005). We therefore constructed an *E. coli* strain, eCOMB (*E. coli* for combing), that incorporates BrdU with a dramatically enhanced efficiency.

Here we report how, using the DNA-combing method with the eCOMB strain, we accurately determined the distribution of fork speeds in *E. coli* cells. We also provide clear evidence that the DNA chain elongation by Pol III provides a major driving force for fork movement in the cells.

Results

Construction of eCOMB for DNA combing

Difficulties in pulse-labelling of *E. coli* chromosomal DNA with halogenated thymidine analogues have made the DNA-combing approach unsuitable for the study of DNA replication in this model organism. An *E. coli* cell lacking thymidylate synthase (Δ *thyA*) has no reaction pathway for *de novo* synthesis of dTMP but can convert thymidine supplied in a medium to dTMP by using the pyrimidine salvage pathway (Kornberg and Baker, 1992; Ahmad *et al.*, 1998). Halogenated analogues of thymidine can similarly be converted to halogenated analogues of dTMP. We expected that two genetic determinants, *deoCAB* and *yjiG*, would affect incorporation of the analogue in *thyA*-deleted MG1655 (MK7158; Table S1). *deoCAB* functions in thymidine catabolism (Ahmad *et al.*, 1998) and *yjiG* prevents incorporation of non-canonical pyrimidine nucleosides (Titz *et al.*, 2007) (Fig. S1). To eliminate these genes, we introduced in the MK7158 strain a 12 kb deletion spanning from *yjiG* to *deoCAB*, resulting in eCOMB (Table S1).

As shown in Fig. 1A, the eCOMB cells incorporated BrdU 18-fold faster than the 15T⁻ cells (Roepke *et al.*, 1944). When the growth medium had a low concentration of thymidine (2 µg ml⁻¹), the growth rate, cell shape and nucleoid structure of the eCOMB cells were indistinguishable from those of the wild-type MG1655 cells (Fig. S2A–D). In the presence of a high concentration of BrdU (50 µg ml⁻¹) for up to 30 min, the cell was not elongated. The initial rates of nucleotide incorporation (within 16 min) into eCOMB cells were similar in measurements with BrdU and radioactive [³H] thymidine (Fig. 1B). These results show that for at least 16 min there were neither obvious stresses on cell growth nor an apparent inhibitory effect on DNA chain elongation when eCOMB cells were grown with the halogenated analogue.

DNA combing with chromosomal DNA of eCOMB cells labelled with thymidine analogues

Fork speed was examined by pulse-labelling eCOMB cells in a thymidine-free medium sequentially, first with the thymidine analogue CldU for 2 min and then with IdU for 2 min (Fig. 2A). The first labelling with CldU serves to mark ongoing replication forks, while the second labelling with IdU is to monitor the chain elongation rate corre-

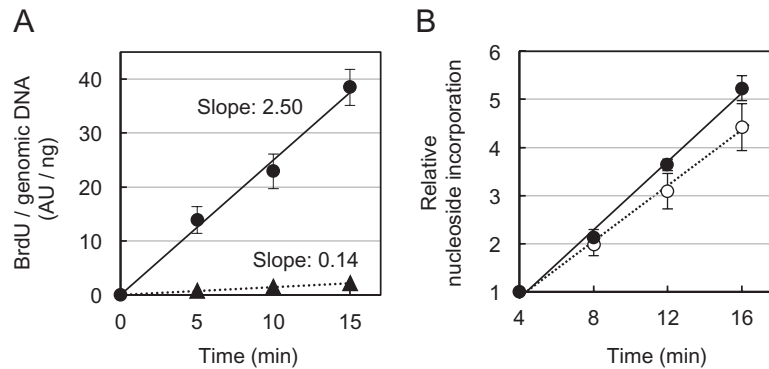


Fig. 1. Efficient incorporation of nucleosides into eCOMB cells.

A. Massive incorporation of BrdU into eCOMB cells. The eCOMB (filled circles) and 15T⁻ (filled triangles) cells were incubated at 37°C in 56/2 medium containing 50 µg ml⁻¹ BrdU.

B. Comparable incorporation of BrdU and thymidine into eCOMB cells. The eCOMB cells were incubated in medium containing either 50 µg ml⁻¹ BrdU (filled circles) or 2 µg ml⁻¹ [³H] thymidine (open circles). In the latter case, the cells were pre-labelled with [¹⁴C] thymidine. Aliquots of cell cultures were withdrawn at each time point and analysed. For the samples labelled with BrdU, chromosomal DNA was extracted and visualized with anti-BrdU antibodies, and the immune-signals (AU; arbitrary units) were quantified with a luminescence image analyser. Radioactivities of ³H and ¹⁴C in an acid insoluble fraction were measured with a scintillation counter. For normalization, the AU values of BrdU signals and counts of [³H] thymidine were divided by the sample DNA amounts (ng) and [¹⁴C] thymidine counts respectively. The normalized values for incorporation of BrdU and [³H] thymidine were expressed relative to those at 4 min in (B). The slope values in (A) were estimated with a linear regression line. Error bars indicate standard errors of the mean (SEM) from three independent experiments; some errors are too small to be seen at the scale of this graph.

sponding to the fork speed. Since exogenously supplied thymidine is incorporated into the chromosomal DNA of *thyA*⁻ cells without prior equilibration with the entire cellular dTTP in a very small pool of dNTP (Pato, 1979; Guzmán *et al.*, 2011), the chromosomal DNA of eCOMB cells could also be pulse-labelled with a high concentration (50 µg ml⁻¹) of the extracellular thymidine analogues promptly after the medium was changed. The SOS response, indicative of replication stress, was not triggered when the exponentially growing eCOMB cells were incubated for 6 min in the presence of IdU (Fig. S2E). We concluded from this that the normal replication fork speed could be measured with eCOMB cells grown in the presence of IdU.

After stretching and denaturing the chromosomal DNA on a glass surface (Fig. S3A), the CldU (red) and IdU (green) regions in the extended DNA fibres were readily detected with two anti-BrdU antibodies (Fig. 2B). The rat anti-BrdU antibody binds to CldU but not to IdU, while the mouse anti-BrdU antibody binds to both CldU and IdU. Denatured DNA molecules on the coverslips were incubated first with the former antibody to saturate CldU sites and then with the latter antibody to selectively react with IdU. About one-third of the labelled DNA fibres were dual-labelled molecules (Fig. S4A). To determine the fork speed, we selected the ones having an IdU stretch lined up with a CldU stretch end-to-end (Figs 2C and S4B), which ensures that the IdU-labelled DNA chain was synthesized at the single replication fork underway throughout the labelling time with IdU. The labelling patterns of

both CldU and IdU were sparse, probably because of incomplete denaturation of dsDNA; the anti-BrdU antibodies react with the thymidine analogues in ssDNA.

Solitary yellow dots were often contained in the red and green stretches, and a very short yellow track was sometimes detected in the transition region from red and green stretches (Figs 2C and S4B). The yellow signals were caused by overlapping of red with green signals probably due to incomplete occupancy of the rat antibody at the CldU sites. It is also likely that when a small amount of CldUTP was present in the dNTP pool of *E. coli* cells during the pulse-label with IdU, incorporation of CldU and IdU very near to one another in DNA produced the yellow signals in green stretches. Because of the difficulty of strictly distinguishing between these two possibilities for each yellow signal, we generally ignored the yellow signals. We defined the length of IdU-labelled DNA as the distance between the first and last green foci adjacent to the red stretch. Exclusion of the yellow track in the measurement of the green stretch could lead to a slight underestimation of fork speed determined in the 2 min incubation with IdU. To assure independence of the DNA fibres, we omitted molecules with a gap larger than an about 10 kb in the IdU stretch. To determine fork speed, we measured the actual length of the DNA microscopically and, with lambda DNA as the standard, converted it to the number of nucleotides (Fig. S3B and F). As described below, data obtained with the eCOMB strain and the double-labelling protocol were reproducible and reliable for estimating the fork speed in *E. coli* cells.

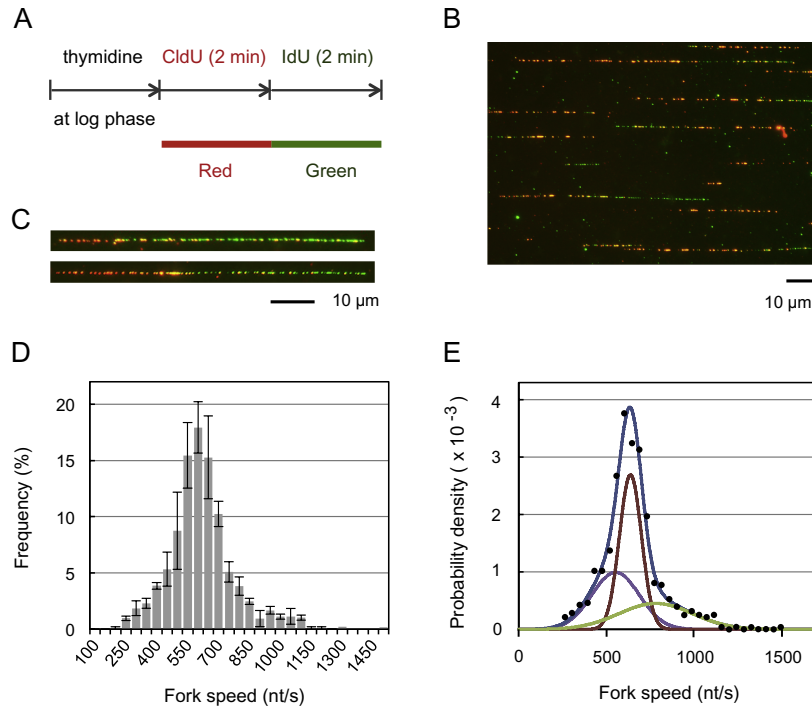


Fig. 2. Distribution of replication fork speed in eCOMB cells.

A. The experimental diagram of DNA double-labelling. The eCOMB cells were pulse-labelled sequentially, first with CldU (red) for 2 min and then with IdU (green) for 2 min.

B and C. Combed DNA fibres. A representative image observed with a fluorescence microscope is shown in (B). The representative DNA molecules used for determination of fork speed are shown in (C). The black bar below each image corresponds to 10 μm .

D. Distribution of fork speeds. Fork speed was calculated from the length of IdU tracks in combed CldU-IdU DNA. Error bars are the SEM for the data from three independent experiments. The total number of DNA fibres analysed was 667. The frequency of the replication fork at speeds ranging from 550 to 750 nt s^{-1} was 58.9%.

E. Fitting of the mixed Gaussian curve to the fork-speed distribution. The fork-speed distribution in (D) was converted to probability density (filled circles), and then the number of Gaussians was determined by using the Akaike Information Criterion. The data were best-fitted to the mixed Gaussian distribution (blue line) consisting of the three Gaussian curves shown by purple, brown and green lines with means of 553, 638 and 782 nt s^{-1} and mixing proportion of 34%, 42% and 24% respectively.

Distribution of replication fork speeds in exponentially growing *E. coli* cells

Figure 2D shows a frequency histogram of 667 replication fork speeds measured in three independent labelling experiments. The measured DNA lengths of the IdU tracks ranged from 30 to 180 kb with a mean of about 77 kb (Fig. S3E). Frequency histograms of the lengths of entire DNA molecules stained with YOYO-1 on glass slides had no obvious peaks (Fig. S3C and D). The distribution profile of individual replication forks had a single peak with a mean of 644 nt s^{-1} (Fig. 2D); bootstrap analysis indicated that the 95% confident interval of the mean was 632–656 nt s^{-1} (Fig. S5A). About 60% of the replication forks moved at speeds within a relatively narrow range, 550–750 nt s^{-1} , indicating that speed of the fork *in vivo* is rather uniform (Fig. 2D). These observations are consistent with the fork speeds previously estimated by analyses of bulk DNA synthesis in *E. coli* cells (Khodursky *et al.*, 2000; Breier *et al.*, 2005; Odsbu *et al.*, 2009;

Tehranchi *et al.*, 2010; Atkinson *et al.*, 2011), although such bulk analyses provided only an average speed of replication forks. Our single-molecule analysis, however, revealed the presence of replication forks moving much slower or faster than the major population, 14% moving at 250–500 nt s^{-1} and 12% moving at 800–1250 nt s^{-1} . Assuming that the speed distribution of a homogeneous replisome population follows a single Gaussian curve (Tanner *et al.*, 2008; Yao *et al.*, 2009), the fork-speed distribution in Fig. 2D was best-fitted to a mixture of three Gaussian curves (Figs 2E and S5C). This suggests multiple subpopulations of replication forks in the cell. Taking into account numerous natural obstacles on chromosome that affect progression of replication forks (Mirkin and Mirkin, 2007), we think that the subpopulations may be a consequence of replisome dynamics under stressed conditions in growing cells. It was reported that in experiments in which the *in vitro* movement of individual replisomes catalysing coupled replication of both strands was measured in 200–400 s at 23°C, the fork speed of

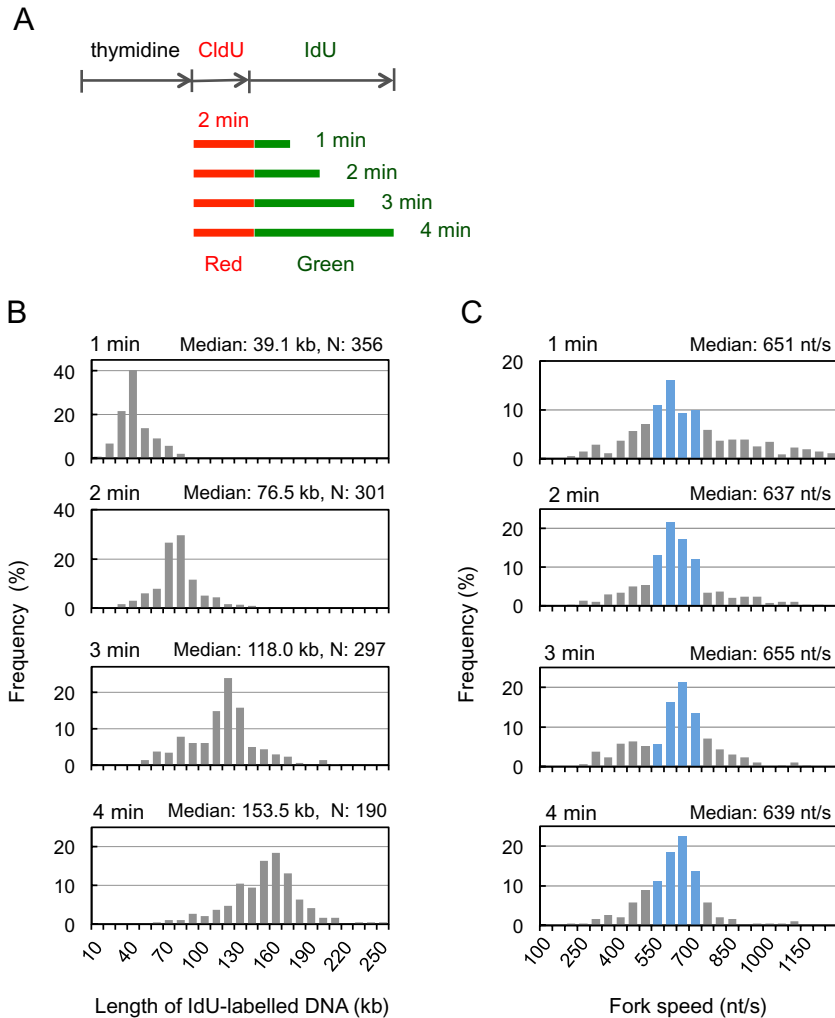


Fig. 3. Time-dependent progression of the replication fork in eCOMB cells.

A. Diagram of DNA labelling in a time-course manner. The eCOMB cells were pulse-labelled with CldU (red) for 2 min followed by with IdU (green) for 1, 2, 3 and 4 min.

B. Distribution of IdU-labelled chromosomal DNA length in a time-course experiment. The double-labelled DNA was extracted from cells collected at each time point and was subjected to DNA combing. The IdU-track lengths in the dual-labelled molecules were measured and shown here in histograms. The median value and the number of DNA molecules observed (N) are shown above each panel.

C. Distribution of fork speed. Fork speeds were calculated from the DNA length at each time point in (B), and the median values are shown above each panel. At 1, 2, 3 and 4 min, 46.5%, 63.8%, 56.6% and 65.8%, respectively, of the replication forks had speeds between 550 and 750 nt s^{-1} (blue bars).

each replisome was constant but differed significantly between replisomes (Yao *et al.*, 2009). According to this observation, it seems likely that a single Gaussian distribution of fork speeds in each subpopulation (Fig. 2E) could be due to the intrinsic but different nature of individual replication forks *in vivo* at 37°C.

Accurate determination of the replication fork speed in *E. coli*

To verify the fork speed determined by the DNA-combing method shown in Fig. 2D, we examined two types of time delays that, because of the very short labelling time, could cause the fork speed to be underestimated: lags in the import of IdU and in the conversion of IdU to IdUTP. To get better time resolution, we labelled newly synthesized DNA in eCOMB cells in 1 min intervals for 4 min after CldU-labelling for 2 min (Fig. 3A) and measured the lengths of IdU-labelled DNA molecules recovered at each time point (Fig. S4). A net increase in the DNA length was propor-

tional to the pulse-labelling time (Fig. 3B). To remove negative effects of outliers in the dataset, the median length at each time point was plotted as a function of time and analysed by linear regression in three independent experiments (Fig. 4A–C). The straight lines through the origin clearly indicate that the time delay in import and conversion of IdU was negligible. The chain elongation rate was determined from three slope values in order to eliminate the possibility of underestimation due to degradation of IdU-labelled DNA during DNA preparation in the DNA-combing procedures. The linear regression coefficients indicated a very high reliability in each slope determination. The three slope values were very close, and the average fork speed in *E. coli* cells growing at 37°C was calculated to be $653 \pm 9 \text{ nt s}^{-1}$ (mean \pm SEM) (Fig. 4D). This speed is within the 95% confidence interval of the average fork speed shown in Fig. 2D (Fig. S5B). This also indicates that omitting the yellow signals when measuring the IdU tracks had little effect on the average fork speed in Fig. 2D.

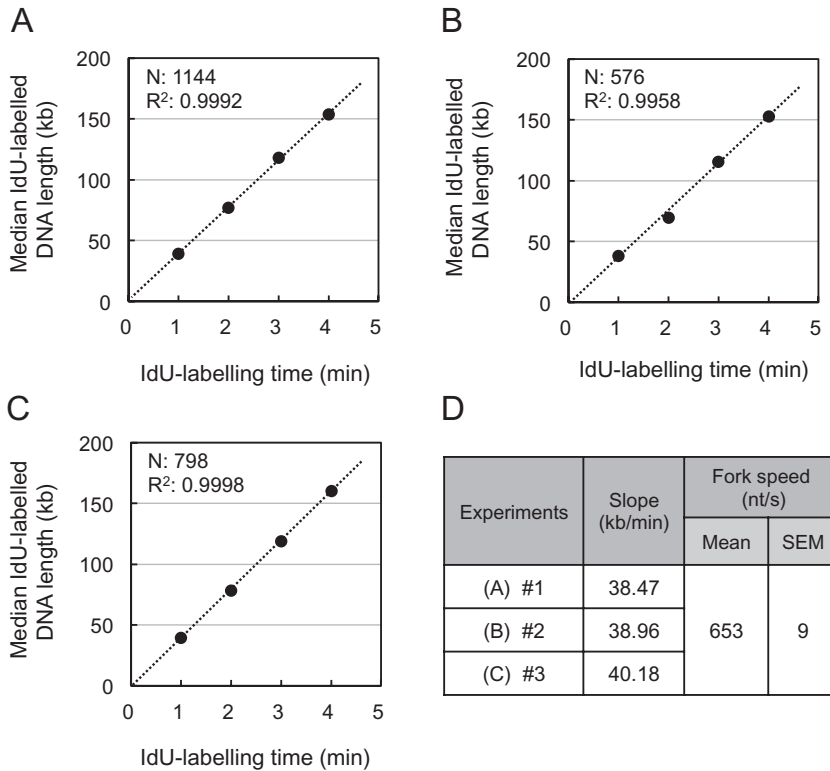


Fig. 4. Accurate determination of replication fork speed. The eCOMB cells were pulse-labelled with CldU for 2 min followed by labelling with IdU in 1 min intervals up to 4 min in triplicate. Experiment #1 (the same sample as Fig. 3), #2 and #3 are shown in (A), (B) and (C) respectively. Median value of IdU-labelled chromosomal DNA length is plotted at each time point. The numbers (N) are the total numbers of DNA fibres observed in each experiment. The broken lines are linear regression lines determined by the least-squares method, and the R² values are coefficients of determination. (D) Determination of fork speed. The mean speed and SEM were calculated from the three slope values of (A), (B) and (C). The total number of DNA fibres observed was 2518.

The distribution of fork speeds at each time point in the representative time-course experiment is shown in Fig. 3C. In all the samples recovered at different time points, about 50–70% of the replication forks were in the moderate subpopulation, with speeds ranging from 550 to 750 nt s⁻¹ (blue bars in histograms). Although the subpopulation of faster replication forks seemed slightly increased at the 1 min time point, the overall profiles of the distributions were the same at each time point. The increase in the faster replication forks at the 1 min time point was not reproduced in the other experiment (Fig. S5D). Therefore, replication forks continued to proceed with a similar average fork speed at least within 200 kb DNA segments replicated in 4 min.

Pacemaking of the replisome progression by DNA polymerase III

It has been postulated that the leading strand synthesis catalysed by Pol III could be a pacemaker that controls replication fork progression (Patel *et al.*, 2011), but no direct evidence for this hypothesis has been provided. Pol III is composed of three subassemblies: the Pol III core (a heterotrimer of α , ϵ and θ subunits), the DnaX clamp-loading complex and the sliding β clamp (Maki and Furukohri, 2013). The *dnaE* gene encodes the catalytic α -subunit of Pol III holoenzyme (Maki *et al.*, 1985). Maki and his colleagues previously isolated a *dnaE173* mutant

strain that produces an altered Pol III with remarkable enzymatic characteristics (Maki *et al.*, 1991). The most striking is that the rate of DNA chain elongation by the *dnaE173* Pol III holoenzyme is greatly reduced to 300 nt s⁻¹, one-third of that observed with the wild-type Pol III holoenzyme *in vitro* (Sugaya *et al.*, 2002). If the Pol III holoenzyme is the pacemaker for the replication fork to move, the fork speed in the *dnaE173* cells should be close to one-third of that in the control cells. As shown in Fig. 5A and B, this is indeed the case. Two derivatives of the eCOMB strain, *dnaE173 Tn10* eCOMB (MK7928) and *dnaE⁺ Tn10* eCOMB (MK7927) as a control, were constructed (Table S1) and analysed for their fork speeds at 37°C by the DNA-combing method. In the *dnaE173* cells, the speed of the majority of the forks (80%) was in the range from 200 to 400 nt s⁻¹, which is greatly shifted to the slower side compared with the range including the speeds of 80% of the forks in the control cells (Fig. 5A). The mean fork speed determined from data obtained in three independent time-course experiments (Fig. S6) was 264 ± 9 nt s⁻¹ in the *dnaE173* cells and 656 ± 10 nt s⁻¹ in the *dnaE⁺* cells (Fig. 5B), indicating that the forks in the former cells proceed at 40% of the speed of the forks in the latter cells. The relative reduction is close to the one (33%) expected from the slow chain-elongation rate of the *dnaE173* Pol III holoenzyme. We therefore concluded that the speed of the replication fork in the *dnaE173* cells was reduced almost proportionally to the slow rate of the DNA

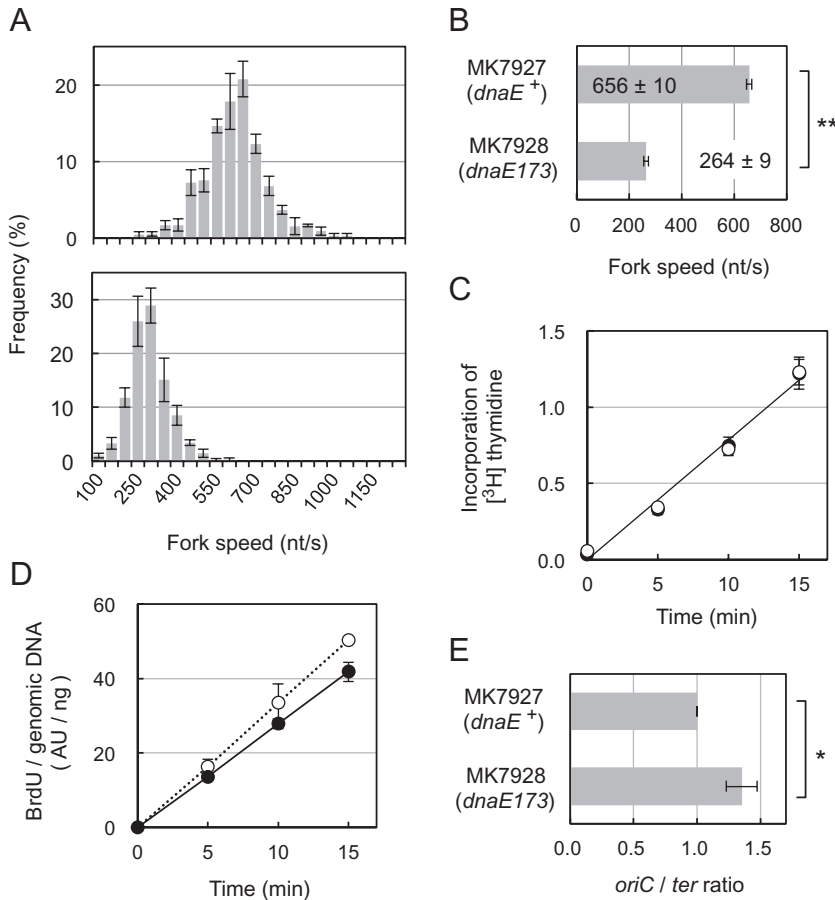


Fig. 5. Slow fork speed in *dnaE173* cells.

(A) Distribution of fork speed. Fork speed distribution was determined for MK7927 (eCOMB, *zae-502::Tn10*; upper) and MK7928 (eCOMB, *dnaE173, zae-502::Tn10*; lower) cells as in Fig. 2. The total number of DNA fibres analysed was 367 for MK7927 and 512 for MK7928. Error bars are the SEM from three independent experiments (B) Replication fork speed. As described in the legend for Figs 3 and 4, the cells were dual-labelled with CldU followed by IdU. The mean fork speed was verified in three independent experiments as shown in Fig. S6. The total number of DNA fibres analysed was 1638 for MK7927 and 2056 for MK7928. (C, D) Rates of net DNA synthesis. (C) Radioactivity of [³H] thymidine and (D) immune-signals of BrdU were measured in triplicate as described in the legend for Fig. 1 and divided, respectively, by the sample DNA amounts (ng) and [¹⁴C] thymidine counts. The normalized value at each time point is plotted in each graph. Open circles: MK7927. Filled circles: MK7928. (E) *oriC/ter* ratio. The *oriC/ter* ratio in the MK7928 cells growing in 5B/2 medium containing 2 μg ml⁻¹ thymidine was determined using quantitative PCR and normalized relative to that in MK7927 cells. Error bars indicate the SEM from three independent experiments (some are too small to be seen here). The asterisks indicate the *P* values determined in a one-tailed Student's *t*-test (**P* < 0.05, ***P* < 0.005).

chain elongation by the mutant type of Pol III holoenzyme. Although there seems to be several other factors affecting fork speed, it becomes clear that the rate of DNA chain elongation by Pol III is a major determinant of the speed of the replication fork in *E. coli* cells.

Despite having reduced fork speed, the *dnaE173* eCOMB cells grew normally at 37°C with the same average cell mass and doubling time as the *dnaE*⁺ eCOMB cells (Fig. S2D and F). Moreover, the rate of DNA synthesis measured by incorporation of [³H] thymidine in the *dnaE173* cells was exactly the same as that in the control *dnaE*⁺ cells (Fig. 5C). A similar result was obtained with BrdU (Fig. 5D), which together with Figs 1B and 5C excludes the possibility that the fork speed in the *dnaE173* eCOMB cells is reduced in the presence of non-canonical halogenated analogues but not canonical thymidine. *E. coli* cells thus maintain the rate of bulk DNA synthesis, and the resulting cell-division cycle, when the fork speed is reduced. We found that in *dnaE173* cells, the ratio of *oriC* DNA (the replication origin) to *ter* DNA (the replication terminus) was enhanced 1.4-fold compared with that in the *dnaE*⁺ cells (Fig. 5E). Because the *oriC/ter* ratio represents the number of replication forks in cells, this result indicates that the increased number of the slow replication forks in

the *dnaE173* cells contributes to keeping overall DNA synthesis the same extent as that in the *dnaE*⁺ cells.

Discussion

We developed a single-molecule technique to measure replication fork speed *in vivo* with a novel *E. coli* strain, eCOMB (Fig. 1). The technique enabled us not only to measure accurate values for the average fork speed in exponentially growing *E. coli* cells (Figs 3 and 4) but also to find that speed distribution of individual replication fork speeds was relatively uniform but contained three subpopulations that had different speeds (Fig. 2). In addition, analyses of the *dnaE173* mutant strain demonstrated clearly that the rate of DNA chain elongation by Pol III is a major determinant of the fork speed in *E. coli* cells (Fig. 5). Evidence of these subpopulations and for this role of Pol III was not apparent in previous bulk measurements of DNA replication in the cells.

Incorporation of thymidine analogues in eCOMB cells was sufficient for DNA combing

Despite the long history of *E. coli* genetics, there is no strain that incorporates halogenated thymidine analogues

into chromosomal DNA rapidly enough and in sufficient quantity for analysing replication fork speed by the DNA-combing method. eCOMB is the first *E. coli* K12 strain that meets these criteria (Fig. 1). In addition to lacking *thyA*, the eCOMB cells lack 11 genes because of the deletion of the 12 kb chromosomal region spanning from *yjgG* to *deoCAB*. We suspect that the deletion enhances BrdU incorporation by allowing great accumulation of BrdU in the cell. Although the Δ *deoA* cells have lost the degradation of BrdU by thymidine phosphorylase that breaks BrdU down to bromouracil and deoxyribose-1-phosphate (dR-1-P) (Fig. S1), uridine phosphorylase also catalyses the same reaction (Beacham and Pritchard, 1971). The loss of *deoB* in addition to *deoC* blocks the catabolism of dR-1-P. Accumulation of dR-1-P might prevent further degradation of BrdU by a negative feedback inhibition of uridine phosphorylase. eCOMB cells retained normal cell morphology in the presence of BrdU, whereas a *deoB*⁺ derivative showed an elongated cell shape under the same growth conditions, suggesting that Δ *deoB* is also important for reducing cellular stress. Although the physiological substrate of the YjgG protein is unknown, this protein is a house-cleaning nucleoside monophosphate phosphohydrolase that prevents incorporation of the artificial BrdU into DNA (Titz *et al.*, 2007). It is likely that eCOMB cells have an increased concentration of non-canonical BrdUTP because they dephosphorylate less BrdUMP (Fig. S1). It is not clear if deletion of the other seven genes (*prfC*, *osmY* and five hypothetical genes) contributes to the greatly improved ability of eCOMB cells to incorporate BrdU. Despite the great ability of eCOMB cells to incorporate BrdU, both CldU and IdU signals were sporadic on DNA fibres in eCOMB cells (Fig. 2B). The continuity of the immunofluorescent signals was improved by neither disrupting the *ung* gene for uracil DNA glycosylase in eCOMB nor denaturing labelled dsDNA on glass with HCl (data not shown).

Speed of individual replication forks was accurately measured in E. coli cells

It has been difficult to obtain accurate values for the replication fork speeds in *E. coli* cells. eCOMB grows normally in the presence of thymidine and induces no detectable replication stress in the presence of IdU during labelling for DNA combing (Fig. S2). The single-molecule speed of the replication fork in an eCOMB cell growing at 37°C was determined to be 653 ± 9 nt s⁻¹ (\pm SEM) (Fig. 4). In the measurement, the time delay in IdU incorporation and degradation of IdU-labelled DNA during DNA preparation were negligible (Figs 3 and 4). Furthermore, the fork speed is very close to the previously reported ensemble-averaged rates: 550–750 nt s⁻¹ (Khodursky *et al.*, 2000; Breier *et al.*, 2005; Odsbu *et al.*, 2009; Tehranchi *et al.*,

2010; Atkinson *et al.*, 2011). These indicate that we observe a normal fork movement in the eCOMB cells. Our single-molecule speed, however, is lower than the ensemble speed of about 900 nt s⁻¹ measured for the Pol III holoenzyme on a primed ssDNA template at 30°C (Sugaya *et al.*, 2002). This suggests possible restriction of the Pol III translocation in the replisome *in vivo*.

Real-time observations of the single-molecule replication at synthetic fork substrates have revealed that the rate of the *E. coli* replisome movement is 536 ± 39 nt s⁻¹ at 37°C (Tanner *et al.*, 2009) and 246 ± 10 nt s⁻¹ at 23°C (Yao *et al.*, 2009). When the fork speed uncertainty based on the standard error of the mean is considered, our speed determination in the exponentially growing cell at 37°C is as accurate as the single-molecule studies *in vitro*. In contrast, this mean speed in the cell is about 20% faster than that of the reconstituted replisome even at 37°C. This suggests that the speed *in vitro* may be slightly underestimated because the reaction conditions do not mimic the cellular environments exactly. Knowing the actual fork speed in the cell may help further optimize the *in vitro* single-molecule assays.

Speed of replication forks in E. coli cells was relatively homogenous

We found that a majority of replication forks were moving with a relatively uniform speed between 550 and 750 nt s⁻¹ (Fig. 2D). In single-molecule analyses of *E. coli* replisomes reconstituted *in vitro*, individual replisomes showed different intrinsic rates of fork movement that varied as much as fivefold and sometimes even more (Tanner *et al.*, 2008; 2009; Yao *et al.*, 2009). It should be noted that the distribution of fork speeds *in vitro* was flatter than that observed *in vivo* (Fig. 2D). While the reason for the heterogeneous rates of fork movement observed *in vitro* is unknown, we must consider the fundamental differences between DNA replication *in vivo* and DNA replication *in vitro*. The reconstituted rolling-circle DNA replication systems used a very homogeneous DNA template and catalysed DNA synthesis without various DNA transactions other than the basic reactions essential for DNA replication. In contrast, the replisome working in cells replicates a more complex template of chromosomal DNA undergoing various biological reactions. Therefore, it is unlikely that the homogenous fork speed is due to the environment of template DNA *in vivo*. Alternatively, the individual replisomes in *E. coli* cells may differ from the reconstituted ones in such a way that they have an inherent nature leading to more uniform fork speeds. The intrinsic variations of the replisome speed may be reduced in the presence of replication hyperstructures formed by multiple replication-related proteins (Bates, 2008) or in a crowded environment composed of many macromolecules in cells (Akabayov *et al.*, 2013).

Another difference is that between the timescales of the fork speed measurements *in vitro* and *in vivo*. The real-time observation of the leading-strand synthesis at 37°C showed brief pausing events and changes in the elongation rate in 25–50 s (Jergic *et al.*, 2013). Since the fork speed in cells was determined with DNA fibres replicated in 2 min at 37°C (Fig. 2D), we cannot exclude the possibility that the intrinsic variations of the fork speed were averaged out in the longer time range *in vivo* (longer than that *in vitro*). To address this possibility, an additional development is required in the single-molecule approach to the fork speed in *E. coli* cells.

There were multiple subpopulations in the distribution of individual replication fork speeds

Our single-molecule analysis revealed that there were slow, moderate and fast speeds of replication forks in *E. coli* cells (Fig. 2E). In growing *E. coli* cells, the replisome encounters numerous natural obstacles on the 4.6 Mb chromosome: transcription machinery, DNA binding proteins, DNA lesions, unusual DNA structures and torsional stress (Mirkin and Mirkin, 2007). An accessory DNA helicase, Rep, together with UvrD and DinG helicases promotes replication across highly transcribed regions (Guy *et al.*, 2009; Boubakri *et al.*, 2010). The absence of Rep indeed reduces the fork speed by half (Lane and Denhardt, 1975; Atkinson *et al.*, 2011). Even in the absence of exogenous DNA damage, replication is disrupted in more than 15% of *E. coli* cells (Renzette *et al.*, 2005), and a small percentage of the cells experiences spontaneous double-strand breaks (Pennington and Rosenberg, 2007). The replication fork speed is reduced by inhibition of topoisomerases that remove positive supercoils that can accumulate ahead of the ongoing forks (Khodursky *et al.*, 2000). The faster subpopulation of replication forks (Fig. 2E) thus seems to be the one moving with the least replication-stress and reflects the maximum velocity with which the replisome can move. The slower subpopulation, on the other hand, could be subjected to more severe replication stress. It follows then that the main population with medium speed might sustain relatively uniform speed by balancing replication stress with the potential capacity of the replisome and/or with the help of other enzymes.

DNA polymerase III provides a major driving force for the replisome progression

The functional interactions between DNA helicase and DNA polymerase generally increase the speed of DNA synthesis coupled with DNA unwinding *in vitro* (Patel *et al.*, 2011). However, because of difficulties in accurate determination of replication fork speed, it has never been

directly demonstrated that the chain-elongation activity of Pol III holoenzyme drives the replisome in the well-characterized *E. coli* cells. We took an advantage of biochemical properties of the *dnaE173* Pol III holoenzyme that differ from those of the wild-type enzyme in ensemble studies: lack of the proofreading activity, more than 10-fold higher processivity, a reduced K_m for dNTP and a slow rate of the DNA chain elongation (Maki *et al.*, 1991; Sugaya *et al.*, 2002). Using our single-molecule technique *in vivo*, we showed that the fork speed is slowed down to the extent that the chain-elongation rate of *dnaE173*-Pol III is decreased (Fig. 5). Including the τ -subunit that mediates the interaction of the Pol III core and DnaB helicase (Kim *et al.*, 1996), the subunit compositions of Pol III* (Pol III lacking the β clamp subunit) in the wild-type and *dnaE173*-Pol III* enzymes are basically indistinguishable (Sugaya *et al.*, 2002). Because of the hyper-processivity of the *dnaE173* Pol III holoenzyme, there is little chance that instability of the mutant Pol III is the reason for this slowdown. Thus, the simple interpretation of the reduced fork speed in the *dnaE173* eCOMB cells is that the *E. coli* replisome movement *in vivo* is largely due to the slow chain elongation of the Pol III holoenzyme. In ensemble biochemical studies (Indiani *et al.*, 2009), the other *E. coli* DNA polymerases, Pol II and Pol IV, synthesized DNA chains much more slowly than Pol III did and accordingly could form a slow replisome in place of Pol III, which supports our conclusion. The DNA synthesis reaction of the Pol III holoenzyme at replication fork may serve to push the DnaB helicase and increase the helicase's net forward movement by generating a force in the direction of unzipping dsDNA as shown for the T7 helicase (Johnson *et al.*, 2007).

Increased number of the slow replication forks contributes to sustaining the net DNA synthesis rate

The cellular DNA replication rate, the average cell mass and the doubling time of *dnaE173* eCOMB cells were the same as those of *dnaE⁺* eCOMB cells, whereas the replication fork speed of the former cells was much slower than that of the latter (Fig. 5A and B). The increased number of the replication forks seems to compensate for the decreased rate of fork progression in the *dnaE173* cell to some extent (Fig. 5E). A similar observation was previously reported with hydroxyurea-treated MG1655 cells (Odsbu *et al.*, 2009) and Δrep mutant cells (Colasanti and Denhardt, 1987); both also showed a reduction in fork speed. The classical interpretation of these observations is that successive rounds of the cell cycle overlap. In rapidly growing *E. coli* cells, the number of the replication forks is increased by the overlapping of replication cycles in which DNA replication initiates before the previous round is completed (Cooper and Helmstetter, 1968). Under this circum-

stance, when the origin fires with a constant timing but independently of the fork speed, the prolonged time necessary to replicate the entire chromosome due to the slow fork progression could produce more forks on the chromosome in the *dnaE173* cell than on the chromosome in the control *dnaE⁺* cell. Another possible explanation is more frequent initiation of the DNA replication in the *dnaE173* cells. The *dnaE173* cells may sense the fork speed and transmit a regulatory signal that makes the mechanisms initiating chromosomal DNA replication change the timing of origin firing. Some of the feedback controls repressing extra initiation events (Skarstad and Katayama, 2013) may modulate the initiation potential in response to the fork speed. Further studies are needed to evaluate these possibilities.

Experimental procedures

Chemicals and antibodies

The thymidine analogues BrdU and IdU were purchased from Sigma-Aldrich, USA, and the analogue CldU was purchased from MP Biomedicals, USA. [^{14}C] thymidine ($> 50 \text{ mCi mmol}^{-1}$) and [methyl- ^3H] thymidine ($70\text{--}90 \text{ Ci mmol}^{-1}$) were purchased from PerkinElmer, USA. Rabbit anti-RecA antibodies were purchased from Bio Academia, Japan. Mouse and rat anti-BrdU monoclonal antibodies were purchased from Becton Dickinson, USA and Abcam, USA respectively. Anti-IgG antibodies conjugated with Alexa Fluor Dye were purchased from Life Technologies, USA. HRP-conjugated anti-mouse IgG antibodies were purchased from GE Healthcare, USA. Florescent dyes other than 4',6-diamidino-2-phenylindole (DAPI), which was purchased from Dojindo Laboratories in Japan, were purchased from Life Technologies, USA.

Construction of bacterial strains

All *E. coli* strains used are listed in supplementary Table S1. General methods for DNA manipulation and transformation followed standard procedures (Sambrook and Russel, 2001). Cells with the ability to efficiently incorporate BrdU were made by sequentially deleting the *thyA* and *deoB* of MG1655 (Guyer *et al.*, 1981). This was done using P1(*vir*)-mediated transduction (Miller, 1972) with the respective donors, JWK2795 and JWK4346, from the Keio collection (Baba *et al.*, 2006). Following each replacement of the chromosomal genes, the resulting strains were transformed with plasmid pCP20 (Table S2) to eliminate the *kan* (kanamycin-resistant) gene at the flippase recognition target (FRT) by using a site-specific recombinase (Datsenko and Wanner, 2000). The resulting strain was MK7167 (MG1655 ΔthyA ΔdeoB). Next, the DNA fragment carrying $\Delta\text{yjiG}::\text{FRT-kan}$ of JWK4336 was amplified using PCR with the oligonucleotides *yjiG*-F and *yjiG*-R (Table S2). The *yjiG* gene of the MK7167 strain carrying the pKD46 plasmid (Table S2) was replaced with the PCR product using the Red-mediated targeting method (Datsenko and Wanner, 2000), and the region span-

ning from *yjiG* to *deoB* of the resulting MK7426 was eliminated by FRT-specific recombination with pCP20, yielding eCOMB. No undesired cross-recombination at the remaining FRT sites in scar were detected in any strain after the excision of *kan*. The *dnaE173* mutator mutation of MK935 was cotransferred with the tetracycline resistance gene of *zae-502::Tn10* into the recipient eCOMB strain by P1 transduction. Among the tetracycline-resistant transductants, mutator colonies were selected on LB plates containing rifampicin, yielding MK7928. Non-mutator colonies were also selected, resulting in a *dnaE⁺* control strain, MK7927.

Bacterial growth conditions

The 56/2 minimal medium was prepared as described elsewhere (Willets *et al.*, 1969) but without streptomycin. It was routinely supplemented with 0.2% casamino acids and $20 \mu\text{g ml}^{-1}$ tryptophan, and depending on the experiment, either thymidine or a thymidine analogue was added to it. LB and M9 salt were prepared as described elsewhere (Sambrook and Russel, 2001). The eCOMB cells were incubated at 37°C for 12 h in LB medium containing $2 \mu\text{g ml}^{-1}$ thymidine. The cells in the overnight culture were rinsed with five times the original culture volume of M9 salt. The cells were mixed with 15–20 ml of 56/2 medium containing $2 \mu\text{g ml}^{-1}$ thymidine to give an OD_{600} of 0.02 in a 50 ml bioreactor tube (TPP, Switzerland), grown exponentially to an OD_{600} of 0.3 at 37°C with shaking, and then treated appropriately for each experiment.

Labelling experiment with thymidine analogues

The exponentially growing cells were centrifuged at $8500 g$ for 10 min at 20°C . During labelling of the cells with thymidine analogues, the cells were incubated in the dark in 56/2 medium containing the analogue but lacking thymidine. For labelling the cells with BrdU, the harvested cells were suspended in prewarmed 56/2 medium containing $50 \mu\text{g ml}^{-1}$ BrdU to an OD_{600} of 0.1 (designated as time zero), and incubation was continued. For double-labelling experiments with CldU followed by IdU, the cells were suspended in prewarmed 56/2 medium containing $50 \mu\text{g ml}^{-1}$ CldU to an OD_{600} of 0.2 and were incubated at 37°C for 2 min. CldU-labelled cells were collected by filtration with a $0.22 \mu\text{m}$ MF-Millipore Membrane Filter (Merck Millipore, USA) and suspended in prewarmed 56/2 medium containing $50 \mu\text{g ml}^{-1}$ IdU to a cell concentration of $\text{OD}_{600} = 0.1$ (designated as time zero), and incubation was continued. To determine the distribution of fork speeds, cells were pulse-labelled with IdU for 2 min. To estimate fork speed in a time-course experiment, cells were pulse-labelled with IdU in 1 min intervals for 4 min. Cell growth in the presence of IdU was terminated by adding a final concentration of 2% sodium azide to the medium.

Molecular DNA combing and immunofluorescent detection of thymidine analogues

Chromosomal DNA was prepared in agarose gel using plug moulds (Bio-Rad, USA) as previously described (Rayssiguier

et al., 1989). The DNA fibre molecules were stretched on silanated coverslips and processed with minor modifications of a previously reported method (Sugimura *et al.*, 2008). Denatured DNA molecules on the coverslips were incubated first with the rat anti-BrdU antibody BU1/75 and then with the mouse anti-BrdU antibody B44. The corresponding immunocomplexes were detected with Alexa Fluor 555-conjugated anti-rat IgG and Alexa Fluor 488-conjugated anti-mouse IgG respectively, and visualized using an Axiovert 200 M fluorescence microscope (Zeiss, Germany) with a 63× objective and appropriate filters. The coefficient used to convert the measured length of combed DNA (μm) to the number of nucleotides was estimated to be $2.3 \text{ kb } \mu\text{m}^{-1}$ in our experimental condition (see Fig. S3F). The length of the IdU tracks at each time point in time-course experiments was the median value of more than 100 measurements and was used to calculate slope when the medians were plotted as a function of the IdU-labelling time.

Measurement of the DNA synthesis rate using BrdU

BrdU-labelled chromosomal DNA of *E. coli* cells was purified with DNeasy Blood & Tissue kit (Qiagen, USA) and quantified, with dsDNA-specific PicoGreen with lambda DNA as the standard, using a fluorescence microplate reader TriStar LB941 (Berthold Technologies, Germany). DNA was denatured at 99°C for 5 min, chilled on ice for 5 min, and loaded in duplicate on a positively charged nylon membrane (Roche, Germany) by using the Bio-Dot SF blotting apparatus (Bio-Rad). The amount of BrdU-labelled DNA loaded in each well was 10 ng for eCOMB and 100 ng for 15T⁻; for eCOMB, the total DNA amounts at each sample were adjusted to 100 ng with non-labelled chromosomal DNA as the carrier. The membrane filter was incubated with blocking reagent (Roche), and BrdU was detected with the mouse anti-BrdU monoclonal antibody followed by incubation with the HRP-conjugated anti-mouse IgG secondary antibody. Immunoblots were developed with ECL reagents (GE Healthcare) to visualize BrdU-labelled DNA by using the LAS-4000 Mini luminescence image analyser (GE Healthcare). The amount of chemiluminescence material was detected with the image analyser; the average amount of BrdU in duplicate samples on the same membrane was measured and expressed in arbitrary units (AU).

Measurement of the DNA synthesis rate using radioactive thymidine

Cells were grown from an OD_{600} of 0.02 to 0.3 at 37°C in 56/2 medium containing $2 \mu\text{g ml}^{-1}$ thymidine and $[^{14}\text{C}]$ thymidine ($0.2 \mu\text{Ci ml}^{-1}$). After rinsing with M9 salts, the cells were added to prewarmed 56/2 medium supplemented with $2 \mu\text{g ml}^{-1}$ thymidine and $[^3\text{H}]$ thymidine ($1.0 \mu\text{Ci ml}^{-1}$) to obtain an OD_{600} of 0.1 and incubated at 37°C . Aliquots (2 ml each) of the culture were taken and quenched at the indicated times by adding 0.4 ml of ice-cold 50% trichloroacetic acid in 0.25 M sodium pyrophosphate. Acid-insoluble materials were collected on GF/C glass-fibre discs (Whatman, UK) by filtration. The discs were washed with a solution containing 1 M HCl and 0.1 M sodium pyrophosphate and then with ethanol before being air-dried. Filter-retained radioactivity was meas-

ured in an Emulsifier Scintillator Plus (PerkinElmer). For normalization, the incorporation of $[^3\text{H}]$ thymidine was divided by that of $[^{14}\text{C}]$ thymidine indicative of the initial amount of DNA in cells labelled with $[^3\text{H}]$ thymidine.

Quantitative PCR for determining the *oriC/ter* ratio

Quantitative PCR was performed according to the manufacturer's instructions. The SYBR Green I Master kit was used to amplify and quantify the Cp values of the *mioC* and *tus* regions adjacent to *oriC* and *ter*, respectively, with the Light-Cycler 480 system (Roche). PCR reactions for each sample were carried out in triplicate. The reaction mixtures (10 μl) contained a pair of oligonucleotides (5 pmol each, Table S2) and chromosomal DNA (5 ng) of exponentially growing *E. coli* cells purified with the DNeasy Blood & Tissue kit (Qiagen). The resultant Cp ratio of *oriC* and *ter* in *dnaE173* cells was normalized by dividing it by the ratio in the control *dnaE⁺* cells.

Statistical analysis

Student's *t*-test was used to evaluate the differences of the average values in Fig. 5B and E, and Fig. S2E; a value of $P < 0.05$ was considered significant. For the probability density in Fig. 2E, the observed counts in the histogram of Fig. 2D were mixed, converted to a histogram with a 2.2 nt s^{-1} bin width, divided by the total count, and then divided again by the bin width. Therefore, the probability that the DNA has the length in a histogram bin was determined by the rectangle area (height \times bin width). The curve of the probability density was estimated with the mixture model shown in Fig. 2E (McLachlan and Basford, 1988; McLachlan and Peel, 2000). The Akaike Information Criterion was used to determine the number of Gaussians (Akaike, 1973; Burnham and Anderson, 1998). Here, we assume a Gaussian mixture because the DNA length distribution *in vitro* has a Gaussian form (Tanner *et al.*, 2008; Yao *et al.*, 2009). Parameter estimation and model optimization were performed with MATLAB (MathWorks, USA).

Acknowledgements

We thank Dr Thomas M. Conrad (Nara Institute of Science and Technology, Japan) for critical review of the manuscript. We also thank Dr Masahiro Terasawa (RIKEN Center for Developmental Biology, Japan) for helpful discussions about DNA combing. We thank Dr Susan M. Rosenberg (Baylor College of Medicine, USA) for the SMR7467 and SMR7623 strains. Keio collection strains were obtained from the National BioResource Project: *E. coli* (National Institute of Genetics, Japan). This work was supported by Grant-in-Aid for Scientific Research on Innovative Areas (23131518 to H.M.) from The Ministry of Education, Culture, Sports, Science and Technology (MEXT), and Japan Society for the Promotion of Science, Japan (JSPS).

Conflict of interest statement

The authors have no conflicts of interest to declare.

References

- Ahmad, S.I., Kirk, S.H., and Eisenstark, A. (1998) Thymine metabolism and thymineless death in prokaryotes and eukaryotes. *Annu Rev Microbiol* **52**: 591–625.
- Akabayov, B., Akabayov, S.R., Lee, S.J., Wagner, G., and Richardson, C.C. (2013) Impact of macromolecular crowding on DNA replication. *Nat Commun* **4**: 1615.
- Akaike, H. (1973) Information theory and an extension of the maximum likelihood principle. In *2nd International Symposium on Information Theory*. Petrov, B.N., and Csáki, F. (eds). Budapest: Akadémiai Kiadó, pp. 267–281.
- Atkinson, J., Gupta, M.K., Rudolph, C.J., Bell, H., Lloyd, R.G., and McGlynn, P. (2011) Localization of an accessory helicase at the replisome is critical in sustaining efficient genome duplication. *Nucleic Acids Res* **39**: 949–957.
- Baba, T., Ara, T., Hasegawa, M., Takai, Y., Okumura, Y., Baba, M., *et al.* (2006) Construction of *Escherichia coli* K-12 in-frame, single-gene knockout mutants: the Keio collection. *Mol Syst Biol* **2**: 2006.0008.
- Bates, D. (2008) The bacterial replisome: back on track? *Mol Microbiol* **69**: 1341–1348.
- Beacham, I.R., and Pritchard, R.H. (1971) The role of nucleoside phosphorylases in the degradation of deoxyribonucleosides by thymine-requiring mutants of *E. coli*. *Mol Gen Genet* **110**: 289–298.
- Bensimon, A., Simon, A., Chiffaudel, A., Croquette, V., Heslot, F., and Bensimon, D. (1994) Alignment and sensitive detection of DNA by a moving interface. *Science* **265**: 2096–2098.
- Bianco, J.N., Poli, J., Saksouk, J., Bacal, J., Silva, M.J., Yoshida, K., *et al.* (2012) Analysis of DNA replication profiles in budding yeast and mammalian cells using DNA combing. *Methods* **57**: 149–157.
- Boubakri, H., de Septenville, A.L., Viguera, E., and Michel, B. (2010) The helicases DinG, Rep and UvrD cooperate to promote replication across transcription units *in vivo*. *EMBO J* **29**: 145–157.
- Breier, A.M., Weier, H.U., and Cozzarelli, N.R. (2005) Independence of replisomes in *Escherichia coli* chromosomal replication. *Proc Natl Acad Sci USA* **102**: 3942–3947.
- Burnham, K.P., and Anderson, D.R. (1998) *Model Selection and Inference: A Practical Information-Theoretical Approach*. New York: Springer-Verlag.
- Colasanti, J., and Denhardt, D.T. (1987) The *Escherichia coli* *rep* mutation. X. Consequences of increased and decreased Rep protein levels. *Mol Gen Genet* **209**: 382–390.
- Cooper, S., and Helmstetter, C.E. (1968) Chromosome replication and the division cycle of *Escherichia coli* B/r. *J Mol Biol* **31**: 519–540.
- Datsenko, K.A., and Wanner, B.L. (2000) One-step inactivation of chromosomal genes in *Escherichia coli* K-12 using PCR products. *Proc Natl Acad Sci USA* **97**: 6640–6645.
- Funnell, B.E., Baker, T.A., and Kornberg, A. (1986) Complete enzymatic replication of plasmids containing the origin of the *Escherichia coli* chromosome. *J Biol Chem* **261**: 5616–5624.
- Guy, C.P., Atkinson, J., Gupta, M.K., Mahdi, A.A., Gwynn, E.J., Rudolph, C.J., *et al.* (2009) Rep provides a second motor at the replisome to promote duplication of protein-bound DNA. *Mol Cell* **36**: 654–666.
- Guyer, M.S., Reed, R.R., Steitz, J.A., and Low, K.B. (1981) Identification of a sex-factor-affinity site in *E. coli* as $\gamma\delta$. *Cold Spring Harb Symp Quant Biol* **45** (Pt 1): 135–140.
- Guzmán, E.C., Salguero, I., Martín, C.M., Acedo, E.L., Guarino, E., Sánchez-Romero, A., *et al.* (2011) Relationship between fork progression and initiation of chromosome replication in *E. coli*. In *DNA Replication-Current Advances*. Seligmann, H. (ed.). Croatia: Tech, pp. 203–220.
- Higuchi, K., Katayama, T., Iwai, S., Hidaka, M., Horiuchi, T., and Maki, H. (2003) Fate of DNA replication fork encountering a single DNA lesion during *oriC* plasmid DNA replication *in vitro*. *Genes Cell* **8**: 437–449.
- Indiani, C., Langston, L.D., Yurieva, O., Goodman, M.F., and O'Donnell, M. (2009) Translesion DNA polymerases remodel the replisome and alter the speed of the replicative helicase. *Proc Natl Acad Sci USA* **106**: 6031–6038.
- Jergic, S., Horan, N.P., Elshenawy, M.M., Mason, C.E., Urathamakul, T., Ozawa, K., *et al.* (2013) A direct proofreader-clamp interaction stabilizes the Pol III replisome in the polymerization mode. *EMBO J* **32**: 1322–1333.
- Johnson, D.S., Bai, L., Smith, B.Y., Patel, S.S., and Wang, M.D. (2007) Single-molecule studies reveal dynamics of DNA unwinding by the ring-shaped T7 helicase. *Cell* **129**: 1299–1309.
- Khodursky, A.B., Peter, B.J., Schmid, M.B., DeRisi, J., Botstein, D., Brown, P.O., and Cozzarelli, N.R. (2000) Analysis of topoisomerase function in bacterial replication fork movement: use of DNA microarrays. *Proc Natl Acad Sci USA* **97**: 9419–9424.
- Kim, S., Dallmann, H.G., McHenry, C.S., and Marians, K.J. (1996) Coupling of a replicative polymerase and helicase: a τ -DnaB interaction mediates rapid replication fork movement. *Cell* **84**: 643–650.
- Kornberg, A., and Baker, T. (1992) *DNA Replication*. New York: W. H. Freeman and Company.
- Lane, H.E.D., and Denhardt, D.T. (1975) The *rep* mutation IV. Slower movement of replication forks in *Escherichia coli* *rep* strain. *J Mol Biol* **97**: 99–112.
- McHenry, C.S. (2011) DNA replicases from a bacterial perspective. *Annu Rev Biochem* **80**: 403–436.
- McInerney, P., and O'Donnell, M. (2004) Functional uncoupling of twin polymerases: mechanism of polymerase dissociation from a lagging-strand block. *J Biol Chem* **279**: 21543–21551.
- McLachlan, G.J., and Basford, K.E. (1988) *Mixture Models: Inference and Applications to Clustering*. New York: Marcel Dekker.
- McLachlan, G.J., and Peel, D. (2000) *Finite Mixture Models*. New York: Wiley.
- Maki, H., and Furukohri, A. (2013) DNA polymerase III, Bacterial. In *The Encyclopedia of Biological Chemistry*, Vol. 2. Lennarz, W.J., and Lane, M.D. (eds). Waltham, MA: Academic Press, pp. 92–95.
- Maki, H., Horiuchi, T., and Kornberg, A. (1985) The polymerase subunit of DNA polymerase III of *Escherichia coli*. I. Amplification of the *dnaE* gene product and polymerase activity of the α subunit. *J Biol Chem* **260**: 12982–12986.
- Maki, H., Mo, J.Y., and Sekiguchi, M. (1991) A strong mutator

- effect caused by an amino acid change in the α subunit of DNA polymerase III of *Escherichia coli*. *J Biol Chem* **266**: 5055–5061.
- Miller, J.H. (1972) *Experiments in Molecular Genetics*. New York: Cold Spring Harbor Laboratory Press.
- Mirkin, E.V., and Mirkin, S.M. (2007) Replication fork stalling at natural impediments. *Microbiol Mol Biol Rev* **71**: 13–35.
- O'Donnell, M. (2006) Replisome architecture and dynamics in *Escherichia coli*. *J Biol Chem* **281**: 10653–10656.
- Odsbu, I., Morigen, and Skarstad, K. (2009) A reduction in ribonucleotide reductase activity slows down the chromosome replication fork but does not change its localization. *PLoS ONE* **4**: e7617.
- van Oijen, A.M., and Loparo, J.J. (2010) Single-molecule studies of the replisome. *Annu Rev Biophys* **39**: 429–448.
- Patel, S.S., Pandey, M., and Nandakumar, D. (2011) Dynamic coupling between the motors of DNA replication: hexameric helicase, DNA polymerase, and primase. *Curr Opin Chem Biol* **15**: 595–605.
- Pato, M.L. (1979) Alterations of deoxyribonucleoside triphosphate pools in *Escherichia coli*: effects on deoxyribonucleic acid replication and evidence for compartmentation. *J Bacteriol* **140**: 518–524.
- Pennington, J.M., and Rosenberg, S.M. (2007) Spontaneous DNA breakage in single living *Escherichia coli* cells. *Nat Genet* **39**: 797–802.
- Rayssiguier, C., Thaler, D.S., and Radman, M. (1989) The barrier to recombination between *Escherichia coli* and *Salmonella typhimurium* is disrupted in mismatch-repair mutants. *Nature* **342**: 396–401.
- Renzette, N., Gumlaw, N., Nordman, J.T., Krieger, M., Yeh, S.P., Long, E., et al. (2005) Localization of RecA in *Escherichia coli* K-12 using RecA-GFP. *Mol Microbiol* **57**: 1074–1085.
- Roepke, R.R., Libby, R.L., and Small, M.H. (1944) Mutation or variation of *Escherichia coli* with respect to growth requirements. *J Bacteriol* **48**: 401–412.
- Sambrook, J., and Russel, D.W. (2001) *Molecular Cloning, A Laboratory Manual*. New York: Cold Spring Harbor Laboratory Press.
- Skarstad, K., and Katayama, T. (2013) Regulating DNA replication in bacteria. *Cold Spring Harb Perspect Biol* **5**: a012922.
- Sugaya, Y., Ihara, K., Masuda, Y., Ohtsubo, E., and Maki, H. (2002) Hyper-processive and slower DNA chain elongation catalysed by DNA polymerase III holoenzyme purified from the *dnaE173* mutator mutant of *Escherichia coli*. *Genes Cells* **7**: 385–399.
- Sugimura, K., Takebayashi, S., Taguchi, H., Takeda, S., and Okumura, K. (2008) PARP-1 ensures regulation of replication fork progression by homologous recombination on damaged DNA. *J Cell Biol* **183**: 1203–1212.
- Tanner, N.A., Hamdan, S.M., Jergic, S., Loscha, K.V., Schaeffer, P.M., Dixon, N.E., and van Oijen, A.M. (2008) Single-molecule studies of fork dynamics in *Escherichia coli* DNA replication. *Nat Struct Mol Biol* **15**: 170–176.
- Tanner, N.A., Loparo, J.J., Hamdan, S.M., Jergic, S., Dixon, N.E., and van Oijen, A.M. (2009) Real-time single-molecule observation of rolling-circle DNA replication. *Nucleic Acids Res* **37**: e27.
- Tehranchi, A.K., Blankschien, M.D., Zhang, Y., Halliday, J.A., Srivatsan, A., Peng, J., et al. (2010) The transcription factor DksA prevents conflicts between DNA replication and transcription machinery. *Cell* **141**: 595–605.
- Titz, B., Häuser, R., Engelbrecher, A., and Uetz, P. (2007) The *Escherichia coli* protein YjjG is a house-cleaning nucleotidase *in vivo*. *FEMS Microbiol Lett* **270**: 49–57.
- Willett, N.S., Clark, A.J., and Low, B. (1969) Genetic location of certain mutations conferring recombination deficiency in *Escherichia coli*. *J Bacteriol* **97**: 244–249.
- Wu, C.A., Zechner, E.L., and Marians, K.J. (1992) Coordinated leading- and lagging-strand synthesis at the *Escherichia coli* DNA replication fork. I. Multiple effectors act to modulate Okazaki fragment size. *J Biol Chem* **267**: 4030–4044.
- Yao, N.Y., Georgescu, R.E., Finkelstein, J., and O'Donnell, M.E. (2009) Single-molecule analysis reveals that the lagging strand increases replisome processivity but slows replication fork progression. *Proc Natl Acad Sci USA* **106**: 13236–13241.

Supporting information

Additional supporting information may be found in the online version of this article at the publisher's web-site.